Chapter 22
Investigation of Wind Loads on Utility-Scale Seasonal Tilt Solar PV Power Plants

Syed Abdul Mateen and Kiran S. Bhole

Introduction

As all, we know now a day's climate change is a real issue, which is mainly because of environmental pollution. One of the measures to address this issue is the use of renewable energy [1]. The use of a thermoelectric module is one of the renewable sources [2, 3]. The solar system is most adaptable in all other forms of renewable energy systems. The solar industry is growing rapidly in the last 3 years in India. India's solar installed capacity reached 37.62 GW as of 31 May 2020; also India is at fifth position for generating solar energy in the world. Solar energy has various advantages, as it has zero raw fuel costs. It will give you unlimited supply and there are no environmental issues [4]. The substitute to use the fossil fuel is the power generated from the photovoltaic system. Photovoltaic panels are usually mounted on the rooftops of residential or commercial buildings but these systems are generally smaller than ground-mounted PV systems.

Mainly there are three different types of solar module mount structures (MMS). (1) Fixed tilt module mount structure. (2) Single or double axis solar tracker. (3) Seasonal tilt module mounts structure. One of the commonly used is a fixed tilt module mount structure. In fixed tilt MMS, the tilt angle is always fixed. But it produces less energy than other solar module mount structure [5]. Another type is a single or double axis solar tracker. This system is continuously tracking the position of the sun in order to get the maximum energy. These systems have maximum energy output compared with the other solar MMS, but it is very costly system because of the motor driven

S. Abdul Mateen · K. S. Bhole (✉)
Department of Mechanical Engineering, Sardar Patel College of Engineering, Andheri, Mumbai 400058, India
e-mail: kiran_bhole@spce.ac.in

S. Abdul Mateen
e-mail: abdulmateensyed7@gmail.com

S. Kumar and K. P. Rajurkar (eds.), *Advances in Manufacturing Systems*,
Lecture Notes in Mechanical Engineering,
https://doi.org/10.1007/978-981-33-4466-2_22

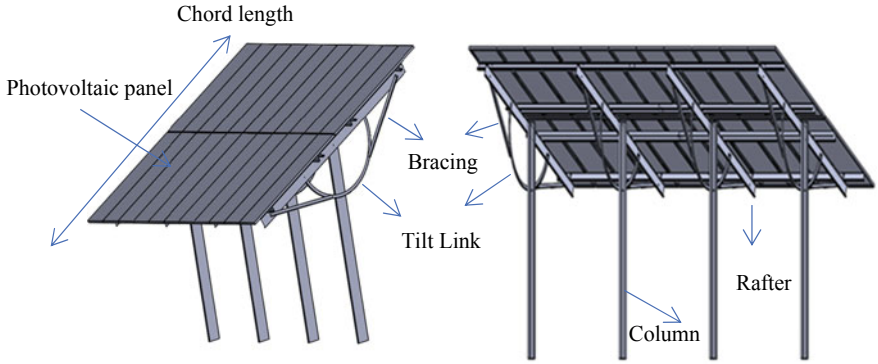

Fig. 22.1 Seasonal tilt module mount structure

tracker unit [6]. Now we will discuss seasonal tilt module mount structure. It provides flexibility in changing the tilt angle of MMS. Depend upon the different seasons and weather conditions, we can change the tilt angle in order to get the maximum energy. Overall PV output can be increased by 5–6% by adjusting the tilt angle twice or thrice a year [7]. The tilt angle ranging from 5 to 40 degrees, and we can simply change the angle using screw jack. Seasonal tilt MMS has many advantages as it is economical, simpler, and durable. It has lower maintenance requirements than a tracking system and stable under extreme weather conditions. That is why we have chosen the seasonal tilt MMS for our analysis.

Seasonal Tilt Module Mount Structure

Solar panels are also called a module, although module is electrical term. Seasonal tilt MMS have series of purlin, tilt link and columns. Modules are rested on the series of purlin and purlin is fixed on rafter as you can see in Fig. 22.1. Tilting links are provided to support rafter and column and used to change the angle of tilt, allowing the rotation of elevation of the PV grid at as 5°, 10°, 15°, 20°, 25°. The Purlins are supported over the rafter. Seasonal tilt MMS is supporting 22 modules. The size of each panel is 1×2 m^2. Modules are placed in portrait position over the Purlin (C-type). Rafters are cold-formed light gauged steel sections and supporting Purlin. Rafters are hinged to the column and braced by bracing member.

CFD Analysis

As we are performing analysis on a utility scale above is our layout for flow simulation. We have leftover one structure in the middle row just to check the effects of

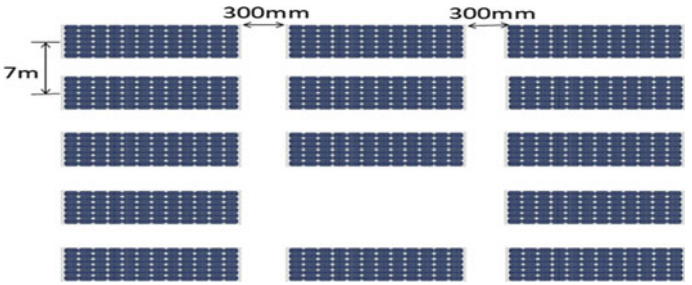

Fig. 22.2 Layout for flow simulation

loads on the surrounding structure. The overall size of the layout is 11 × 32 m^2. The horizontal distance between the two structures is 300 mm and the vertical center to center distance is 7 m. For our analysis purpose, we have chosen five different tilt angles as 5°, 10°, 15°, 20°, 25°. For CFD analysis, we are using Solidworks flow simulation software (Fig. 22.2).

Flow Simulation from Front Side

We are using six different free stream velocities as 33, 39, 44, 47, 50, 55 m/s, these are the Indian standards IS: 875 wind speed, which is used in different regions [8]. In flow simulation for each tilt angle, we have used all six different wind speeds and for each tilt angle at a specific speed, we have calculated normal force acting on the panel. First of all, we have flowed air from the front side and obtain the value of normal forces.

As you can see in Fig. 22.3, a 3D wind tunnel is created in simulation software. The distance between the inlet wall and the first row of the panel is 60 m, and from side walls and back wall it has given a distance of 10 m, also the distance between the

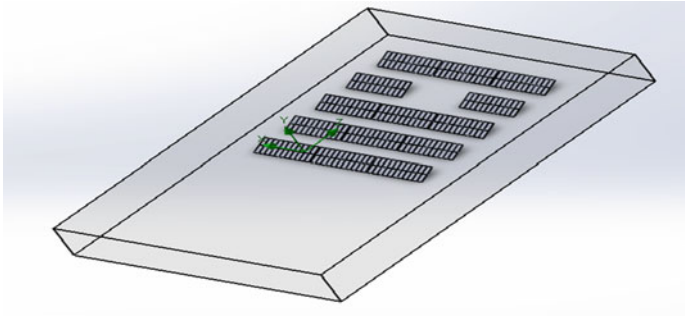

Fig. 22.3 Wind Tunnel under axial load from front side

top and bottom wall is 10 ms. We have fixed all the rows of panels in a fixed plane. We have used global mesh, and the mesh element size is 100 mm. Arrow indicates the air direction.

Results of Flow Simulation

When air flow from the front side, it is found that the maximum normal force is acting on the first row of solar panels as you can see in Fig. 22.4. In Fig. 22.4a, we can see the flow trajectory is of red color on the very first row which means only the first row of panels are experiencing a very large amount of wind loads compared with the remaining rows of panels. Figure 22.4b shows the pressure distribution across the whole panel's layout.

From the graph, we have found that as the tilt angle increase with the increasing wind speed normal force acting on a panel is also going to increase. When air flow from the front side, it is found that the maximum normal force is 1760 N at 25° tilt angle and wind speed of 55 m/s. and minimum normal force is 110 N at 5° tilt angle and wind speed of 33 m/s. It is concluded that wind uplift increases when there is an increase in tilt angle for solar panel.

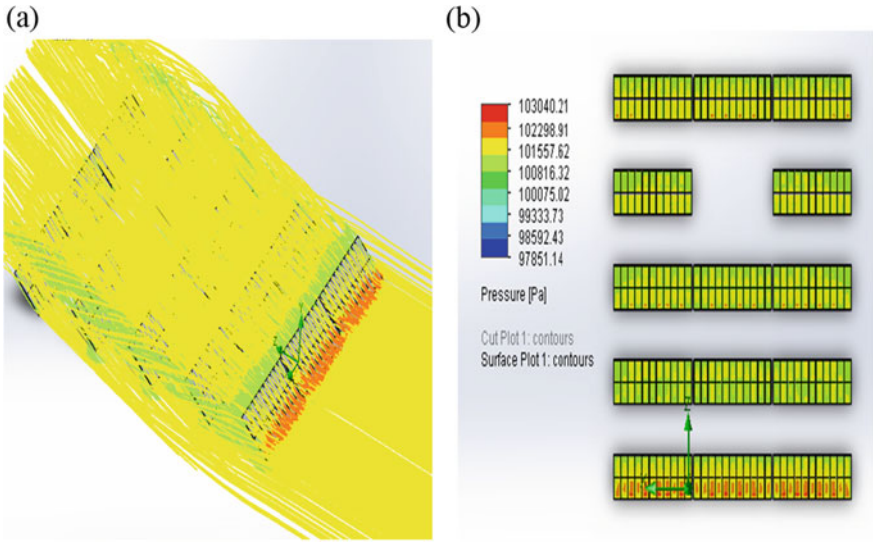

Fig. 22.4 **a** Flow trajectory over panels; **b** Pressure distribution on panel

Flow Simulation from Back Side

When air flow from the backside for each five different tilt angles at six different wind speeds. From this simulation, we have obtained the value of maximum normal force acting on the panels from the backside.

The 3D wind tunnel is created in simulation software as you can see in Fig. 22.5. Arrow indicates the air direction. In the above-created wind tunnel, we have considered clearance of 50 m from both front side and backside and 10 m clearance from the left and right side. The distance between the top and bottom wall is 10 m. We have used global mesh, and the mesh element size is 100 mm (Fig. 22.6).

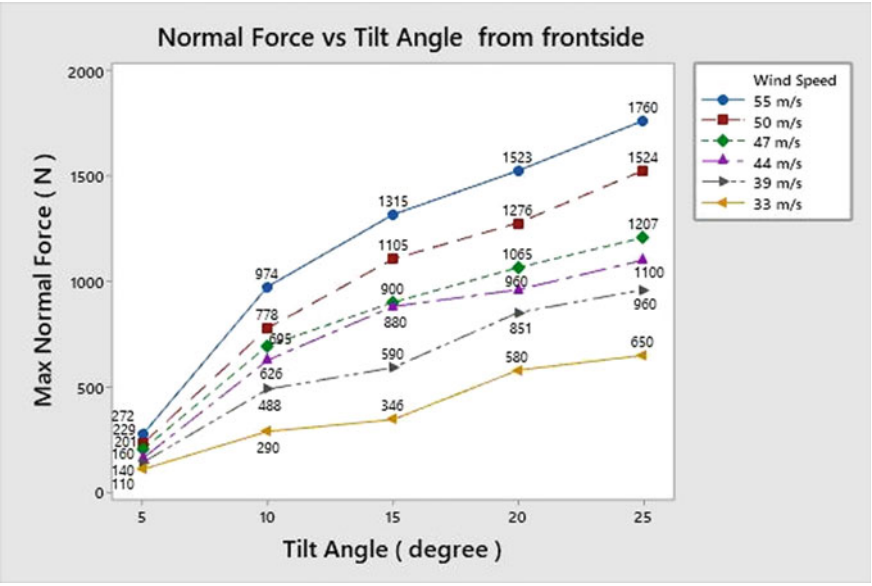

Fig. 22.5 Normal force against tilt angle

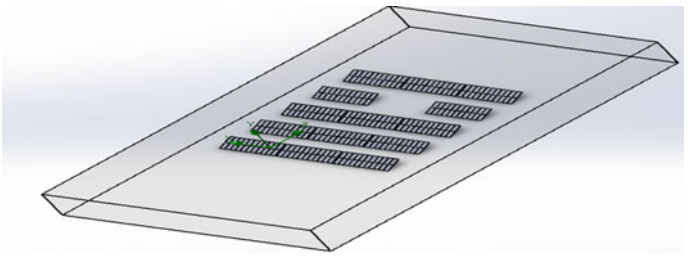

Fig. 22.6 Wind tunnel model under axial wind load

Results of Flow Simulation

When air flow from the back side, it is found that the maximum normal force is acting on the backside of the first row of solar panels as you can see in Fig. 22.7. Figure 22.7a represents the flow trajectory over the panels. Only the first row of panels from the backside is experiencing a very large amount of wind loads compared with the remaining rows of panels. In Fig. 22.7b, red color indicates the maximum pressure acting on the very first row of panels from the backside.

From the graph, we have found that as the tilt angle goes on increasing with the increasing wind speed normal force acting on a panel is also going to increase. When air flow from the backside, it is found that the maximum normal force is 2115 N at 25° tilt angle and wind speed of 55 m/s. and minimum normal force is 103 N at 5° tilt angle and wind speed of 33 m/s.

Flow Simulation at 45° Angle of Attack

When air flow at a 45-degree angle of attack for each five different tilt angles at six different wind speeds. We have chosen a 45-degree angle of attack because panels will face maximum wind load at 45° compared with any other angle of attack ranging from 10° to 80° [9]. From this simulation, we will obtain the value of maximum normal force acting on the panels (Fig. 22.8).

Similarly in this case also 3D wind tunnel is created in simulation software as you can see in Fig. 22.9 and the arrow indicates the air direction. The distance between the top and bottom wall is 10 m. We have used global mesh, and mesh element size is 100 mm.

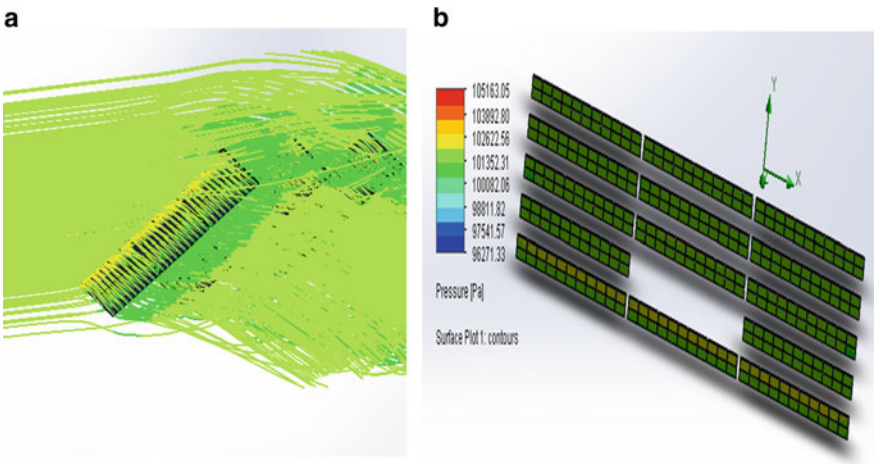

Fig. 22.7 **a** Flow trajectory over panel; **b** Pressure distribution on panel

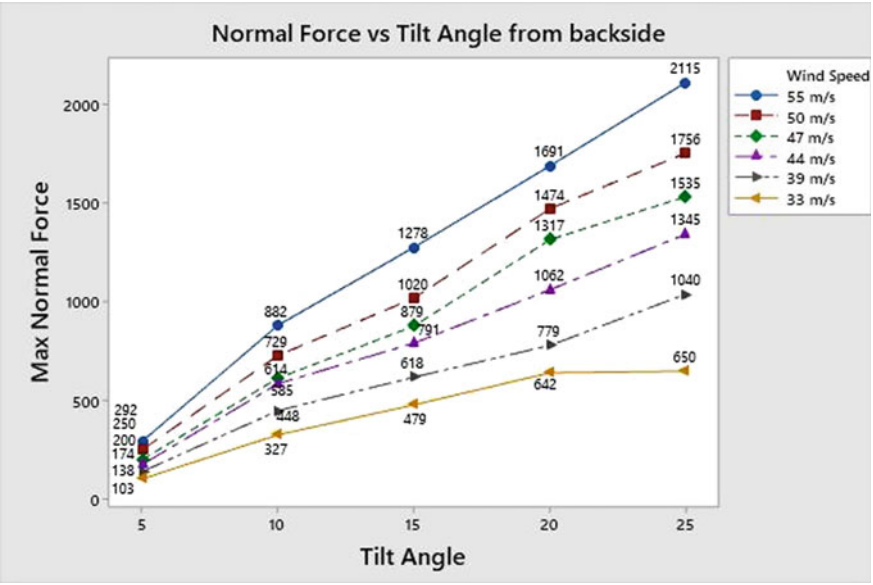

Fig. 22.8 Normal force against tilt angle

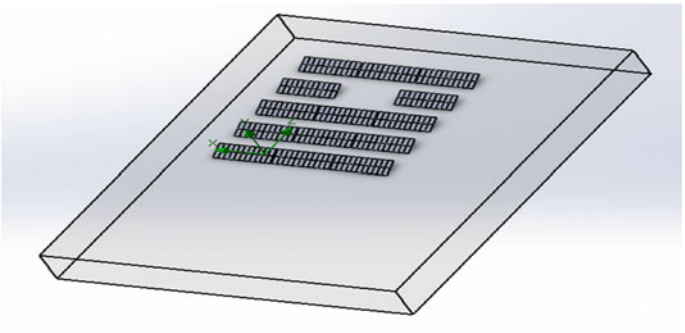

Fig. 22.9 Wind tunnel model for analysis

Result of Flow Simulation

When air flow at 45-degree angle of attack, it is found that maximum wind loads are acting on the first row of panels as well as some side panels of the other rows also which you can see clearly in Fig. 22.10. In Fig. 22.10a, flow trajectory showing the red color are the panels that are experiencing maximum wind loads. Figure 22.10b representing the pressure distribution over the panels. In this case, some panels of each row are experiencing the maximum amount of wind loads (Fig. 22.11).

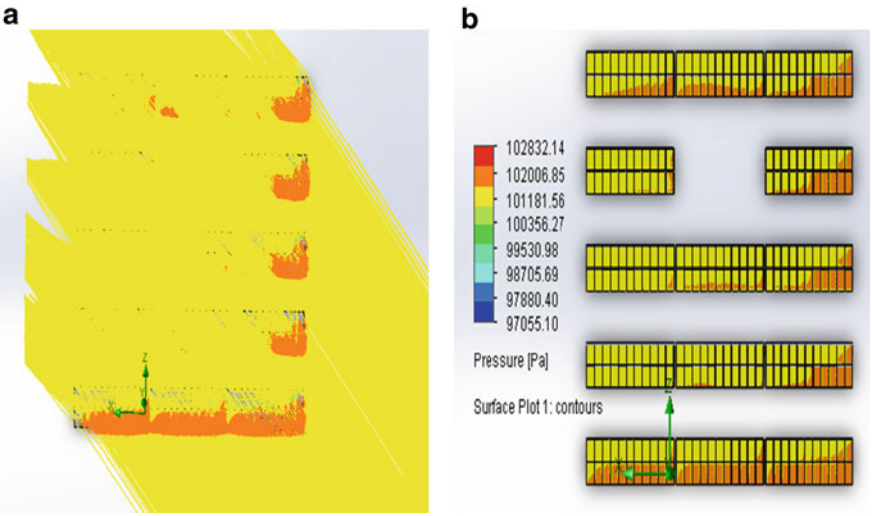

Fig. 22.10 **a** Flow trajectory; **b** Pressure distribution on panel

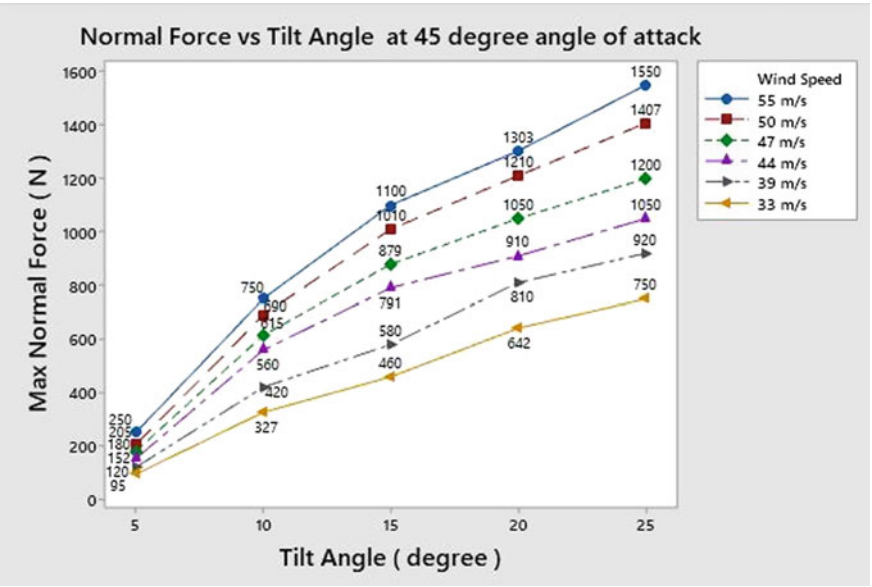

Fig. 22.11 Normal force against tilt angle

From the above graph, we have found that as the tilt angle goes on increasing with the increasing wind speed normal force acting on a panel is also going to increase. When air flow at 45-degree angle of attack, it is found that maximum normal force obtained is 1550 N at 25° tilt angle and wind speed of 55 m/s, and minimum normal force is 95 N at 5° tilt angle and wind speed of 33 m/s.

Static Analysis

This work specifically addresses the Seasonal tilt Module Mounting Structure (MMS) subjected to wind load. The analysis aims to provide the verification of structural stability considering wind for the solar MMS by means of the structural FE analysis. This FE analysis we have done in software called ANSYS. Structural members are considered as homogenous and assumed that they do not contain defects. Rafter to Purlin and Purlin to Module connections are assumed Bonded and Other connections are assumed no-separation. Panel density is 1850 kg m^{-3} and stiffness is 2.1e + 07 N/m^2 [10]. Density and stiffness such that the panel can be considered as a rigid body with mass behavior. Dynamic and static forces exerted on the panel will be directly transferred to purlin without deforming it [11]. Analysis approach using finite element methods has been necessary because of the need to carefully investigate the magnitude of stresses arising from maximum wind loads obtain from flow simulation.

Boundary Conditions and Loads

The analysis aims to provide the verification of structural stability considering wind loads for the solar MMS by means of the structural FE analysis. We have chosen material as a structural steel for analysis. From flow simulation, we obtain a maximum downward force of 1760 N, and the size of each panel is 1×2 m^2. Column's bottom end is constrained in all three directions. Pressure on the panel due to wind loading is applied on the Panel face as normal pressure of 880 Pa. We have considered mesh element size of 25 mm (Fig. 22.12).

Results

We have calculated the von-Mises equivalent stress and total deformation. The static analysis of any module mount structure is done for only supporting structure [12, 13].

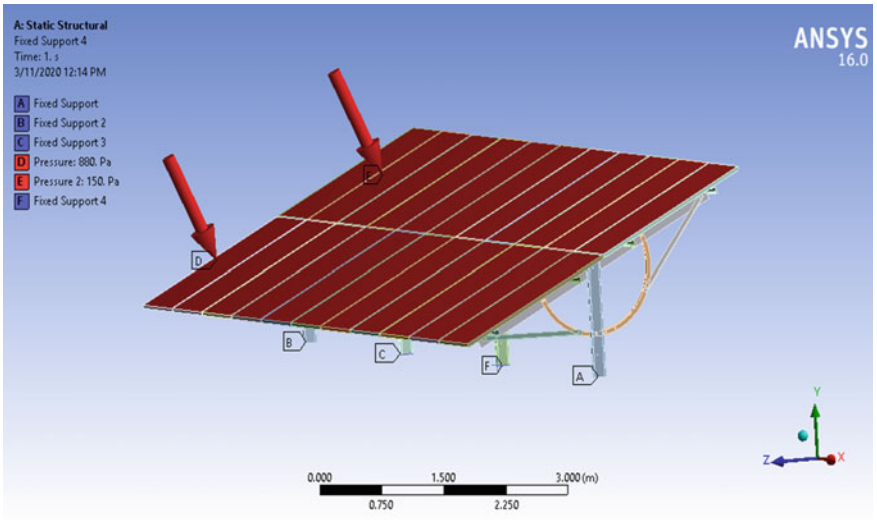

Fig. 22.12 Boundary conditions and loads

Equivalent Stresses Plot

Analysis approach using finite element methods has been necessary because of the need to carefully investigate the magnitude of stresses arising from various wind loads. After applying the maximum downward normal force, we have got the values of equivalent stress. It is seen that when we apply normal force, it will try to downward the structure. From Fig. 22.13, it is found that maximum stress is acting at the joint between purlin and rafter.

Maximum stress = 202 Mpa
Minimum stress = 10559 pa.

Deformation Plot

When we apply maximum normal force obtain from simulation, it is found that maximum deformation is coming at the edge of rafter and minimum deformation is at the bottom of purlin as you can see clearly in the Fig. 22.14.

Maximum deformation = 3 mm.

Conclusion

We have obtained all the values of maximum normal forces at the entire five different tilt angles for six different Indian standard wind speeds. This work carried out to

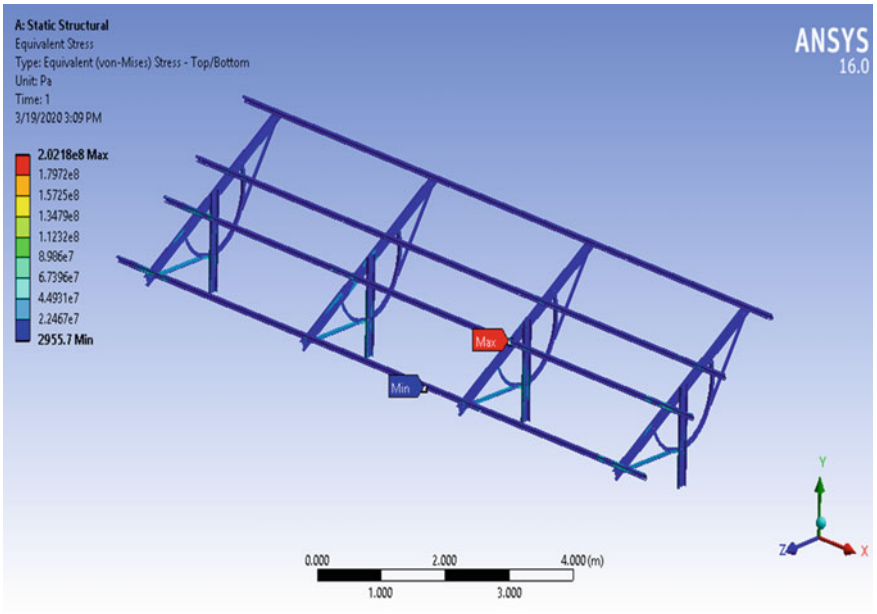

Fig. 22.13 Equivalent stresses plots

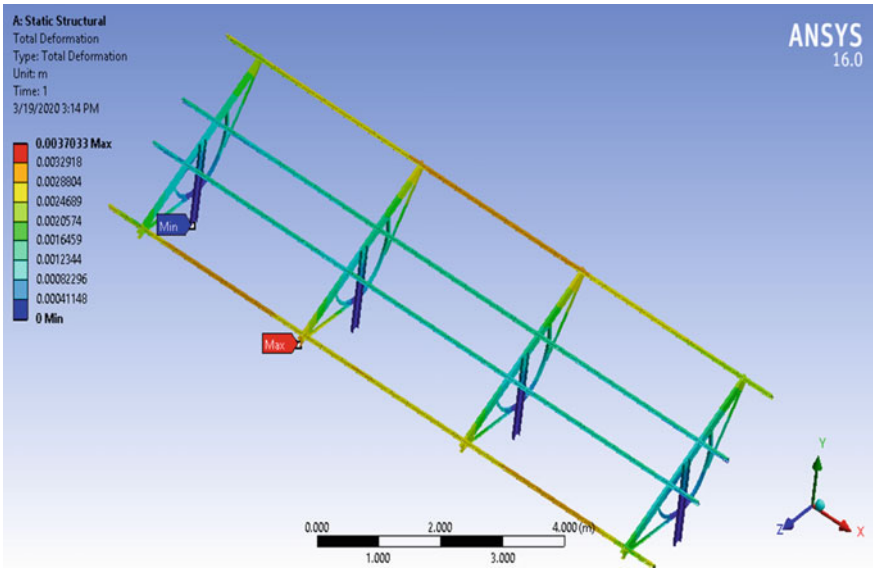

Fig. 22.14 Deformation plot

substantiate assembly of the seasonal tilt PV module mounting structure, which is influenced by wind load obtains from the flow simulation. The work demonstrates that stresses arising in the specified areas are within allowable limits and that the PV module mounting structure is therefore satisfactory for the intended service. Furthermore, we can do an investigation of the dynamic effect on the same seasonal tilt solar PV power plants.

References

1. Cain JH, Banks D (2015) Wind loads on utility scale solar PV power plants. Paper presented at international conference on wind engineering SEAOC convention proceedings
2. Kolambekar RB, Bhole K (2015) Development of prototype for waste heat recovery from thermoelectric system at Godrej vikhroli plant. Paper presented at international conference on nascent technologies in the engineering field (ICNTE)
3. Khadke R, Bhole K (2017) Characterization of radial curved fin heat sink under natural and forced convection. Paper presented at international conference on advances in materials and manufacturing applications (IConAMMA-2017) 17–19, Bengaluru, India
4. Uematsu Y (2007) Wind force coefficients for designing free-standing canopy roofs. J Wind Eng Ind Aerodyn 95:1486–1510
5. Chou C-C (2019) Wind loads on a solar panel at high tilt angles. Appl Sci 9(8):1594
6. Kao-Chun S (2018) Numerical simulation of wind loads on solar panels. Mod Phys Lett B 32(12):1840009
7. Strobel K, Banks D (2014) Effects of vortex shedding in arrays of long inclined flat plate sand ramifications for ground-mounted photovoltaic arrays. J WindEng Ind Aerodyn 133:146–149
8. IS:875 (Part 3–1987), (1989) India standard code of practice for design of loads (other than earthquakes) for buildings and structures, part 3 (wind loads). Bureau of Indian Standards, New Delhi
9. Genc Celik1 G, Celik O (2019) A case study of structural failure of mounting systems for solar panels from south-eastern Turkey: an investigation of design parameters under extreme weather events. Int J Eng Sci Invent 8(1):16–23
10. Chung C (2019) Wind loads on a PV. Array Appl Sci 9(12):2466
11. Camellia A, Milchis T (2019) Wind loading on solar panels. Műszaki Tudományos Közlemények 10:73–78
12. Reina GP, De Stefano G (2017) Computational evaluation of wind loads on sun-tracking ground-mounted photovoltaic panel arrays. J Wind Eng Ind Aerodyn 170:283–293
13. Abiola-Ogedengbe A, Hangan H, Siddiqui K (2015) Experimental investigation of wind effects on a standalone photovoltaic (PV) module. Renew Energ 657–665